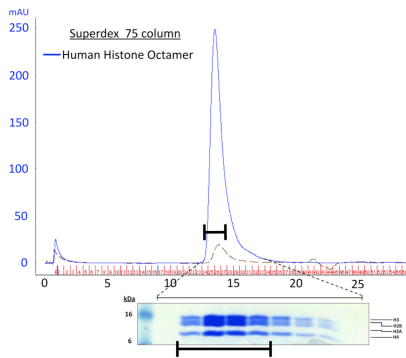
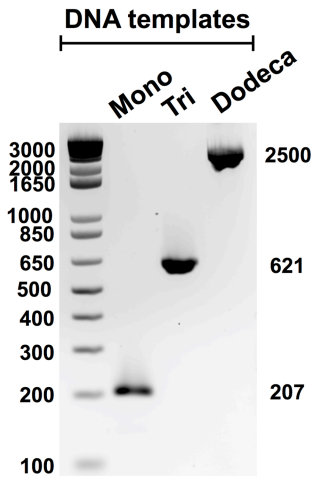
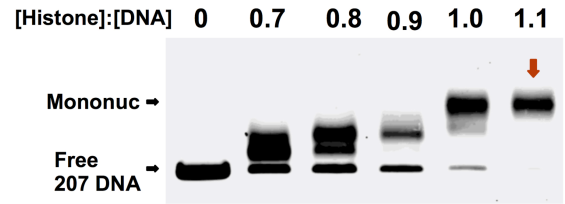
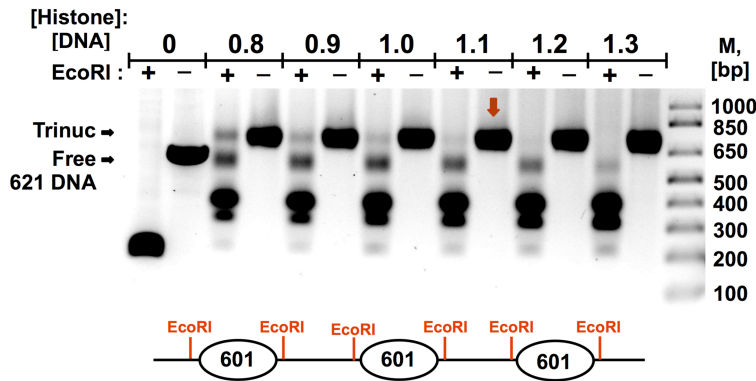
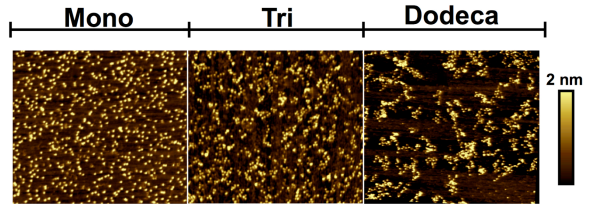
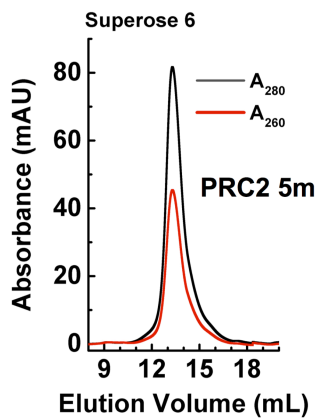
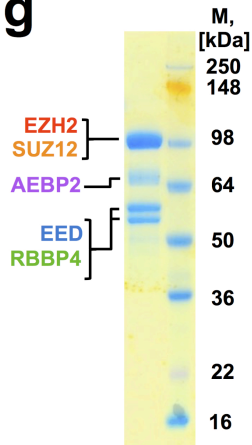
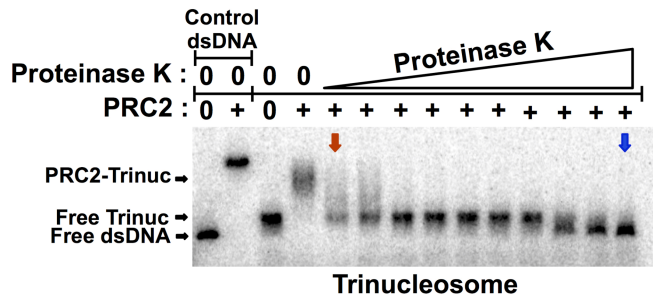
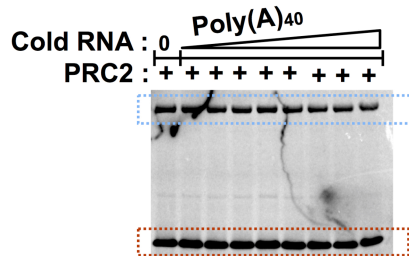
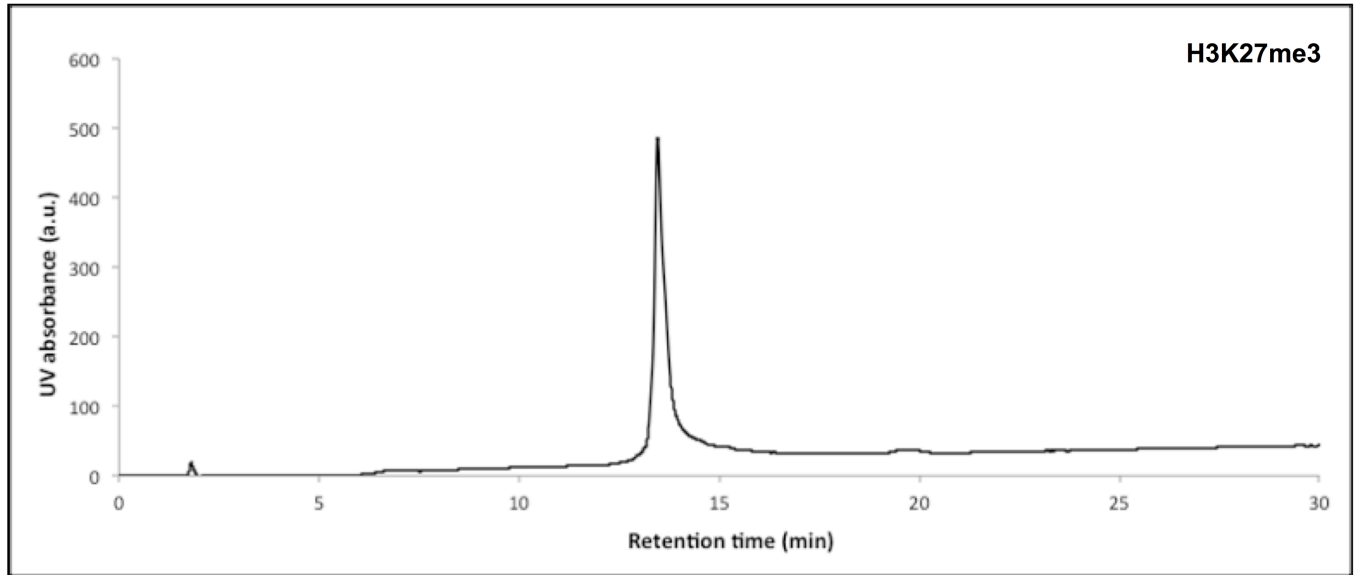
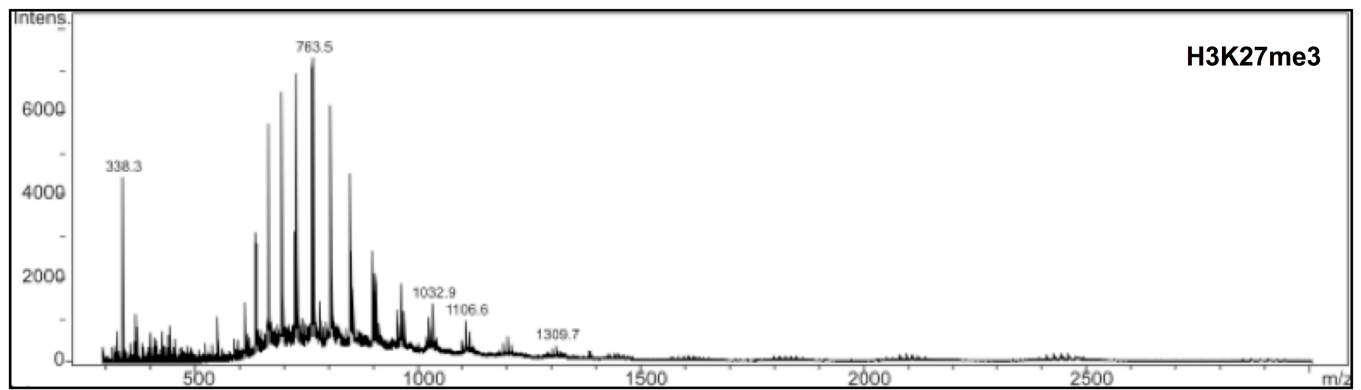
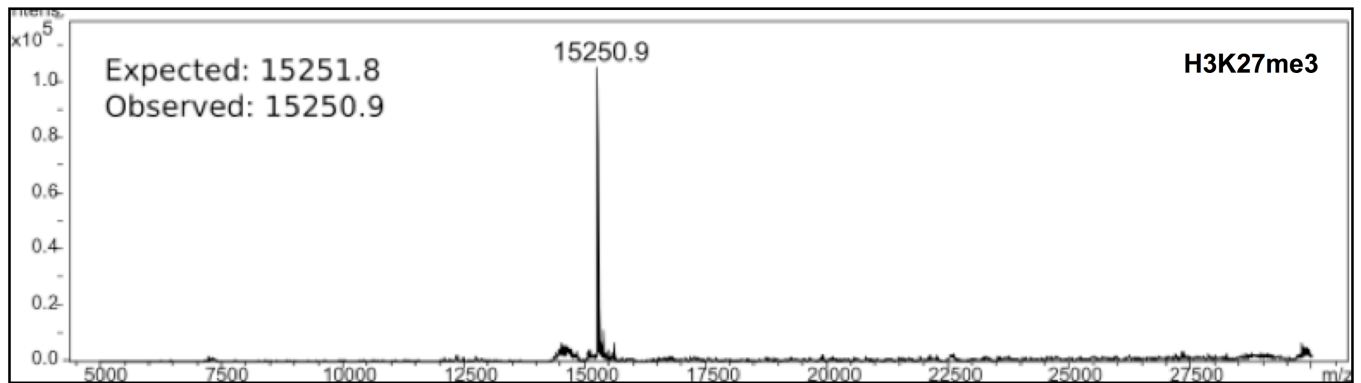


**a****b****c****d****e****f****g****h****i**

## Supplementary Figure 1

### Purification of human PRC2 5-mer complex and its interaction with nucleosomes, Related to Figure 1.

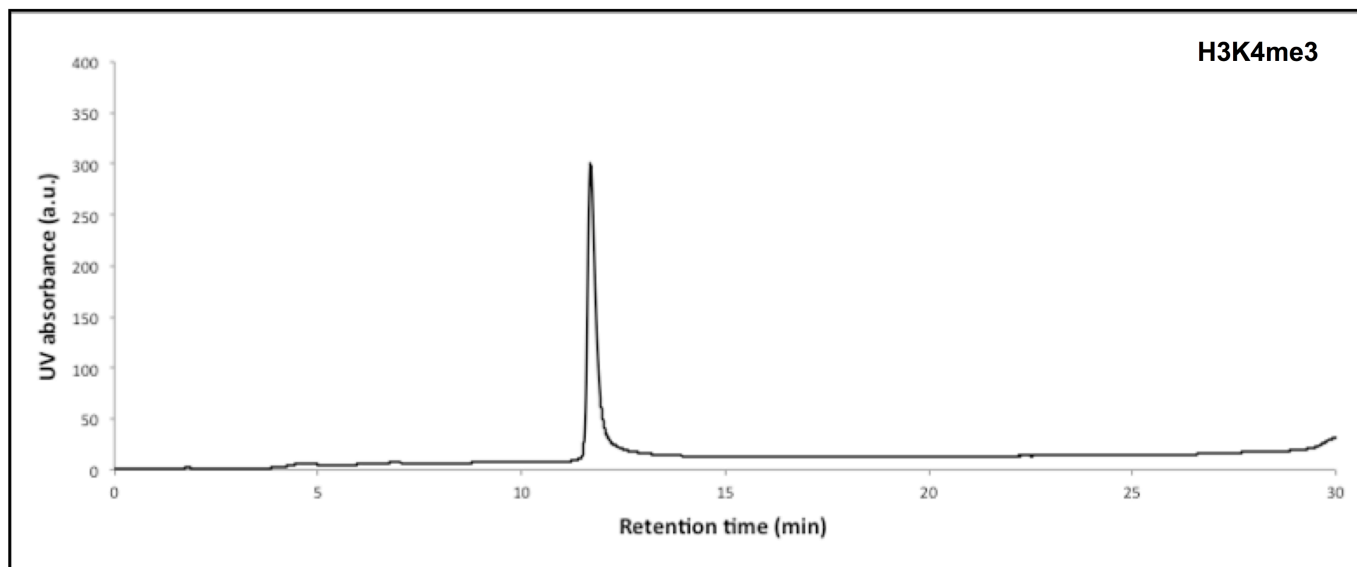
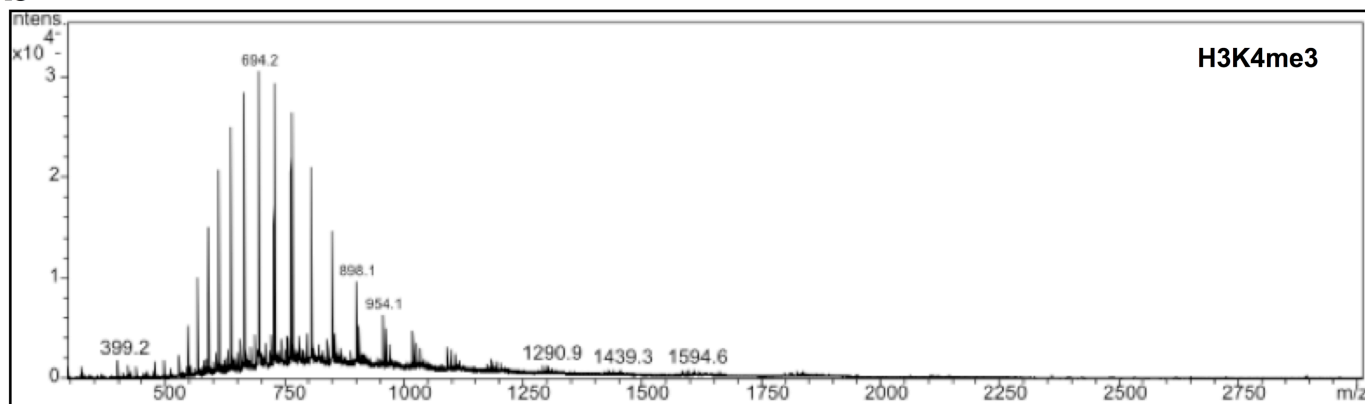
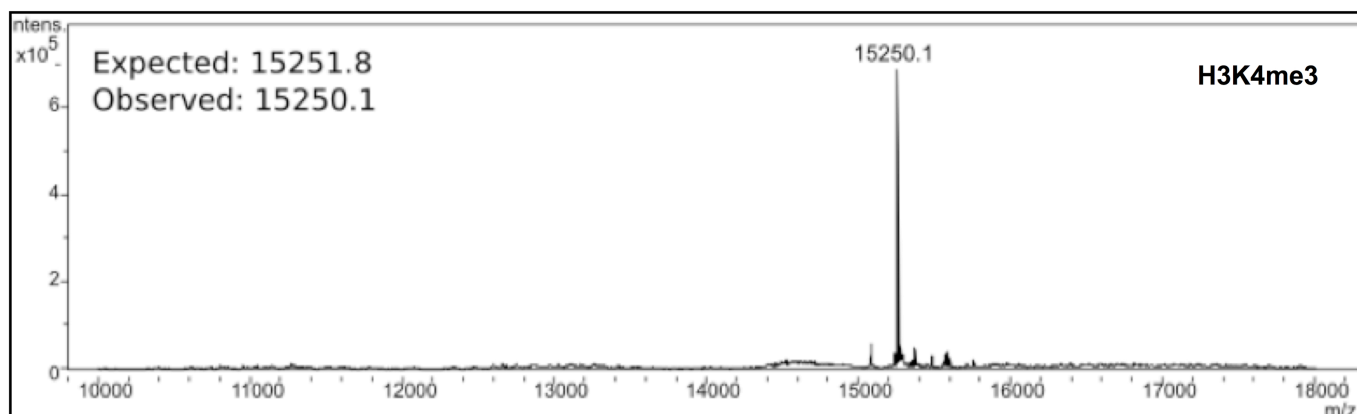
(a) Elution profile of human histone octamer shows that the octamer is monodisperse by size-exclusion chromatography on a Superdex 75 column. Only fractions that had stoichiometric amounts of each histone subunit (1 [H2A]:1 [H2B]:1 [H3]:1 [H4]), as assessed by SDS-PAGE, were pooled, concentrated, and used for nucleosome reconstitution. (b) DNA agarose gel showing the purity of tandemly repeated nucleosome positioning DNA used in the reconstitution of mononucleosomes (207 bp), trinucleosomes (621 bp), and dodecanucleosomes (2500 bp). (c) Representative agarose gel showing the assembly of mononucleosomes as the ratio of histone octamer-to-DNA is increased. In this example, the red arrow indicates a ratio at which mononucleosomes were fully assembled. (d) To ensure that histone octamers were properly assembled on the DNA, preparative gel electrophoresis was performed on trinucleosomes treated with EcoRI. The accessibility of the EcoRI cleavage sites show how saturated the nucleosomes are on the DNA. The red arrow indicates an ideal trinucleosome sample with accessible EcoRI restriction sites. (e) Representative AFM images of mono-, tri-, and dodecanucleosomes shows homogeneity in assembled nucleosomes over a large field of view. (f) PRC2 is monodisperse by size-exclusion chromatography on a Superose 6 Increase column. The lack of nucleic acid contamination is indicated by the A260/A280 ratio < 0.7 and by the absence of staining by ethidium bromide (the latter is not shown here). (g) Purity of a typical PRC2 5-mer complex is assessed by SDS-PAGE. (h) The slow-migrating EMSA band is disrupted by proteinase K treatment (red arrow), confirming that it is a PRC2-nucleosome complex rather than an oligomerization of the nucleosome component stimulated by PRC2. At the highest proteinase K concentration, the trinucleosome band shifted to a free dsDNA band (blue arrow). (i) Histone methyltransferase (HMTase) assays show that Poly(A)<sub>40</sub> RNA does not affect H3K27 methylation. EZH2 automethylation signal is indicated by the blue-dashed box, and H3K27 methylation signal is indicated by the red-dashed box. <sup>14</sup>C-SAM was used as a cofactor in the HMTase reactions. Data points represent 2-fold titrations ranging from 0–60 μM RNA.

**a****b****c**

**Supplementary Figure 2**

**Analysis of semi-synthetic H3K27me3 histone, Related to Figure 2.**

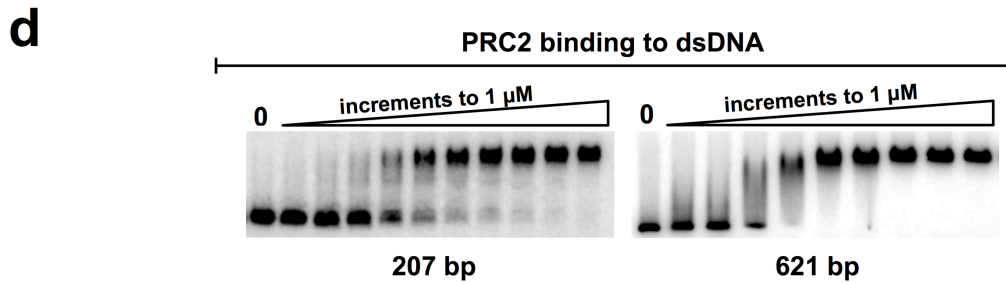
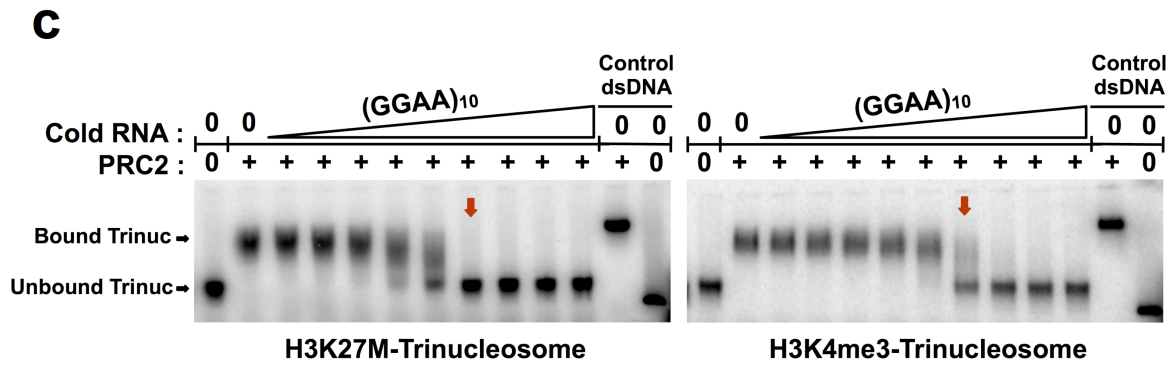
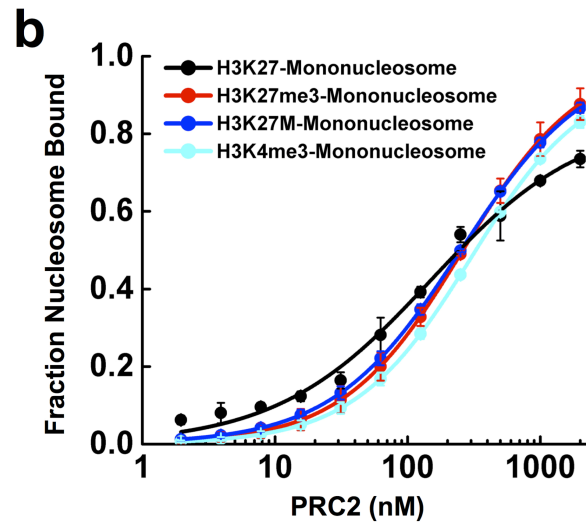
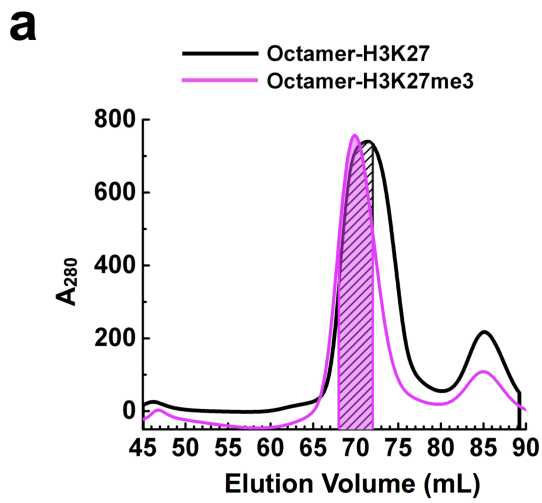
(a) C18 analytical RP-HPLC chromatogram (gradient 0-50% HPLC solvent B) of semi-synthetic of H3K27me3 histone. (b) Corresponding ESI-MS spectrum. (c) Deconvolution of ESI-MS spectrum.

**a****b****c**

### **Supplementary Figure 3**

#### **Analysis of semi-synthetic H3K4me3 histone, Related to Figure 2.**

(a) C18 analytical RP-HPLC chromatogram (gradient 0-50% HPLC solvent B) of semi-synthetic H3K4me3 histone. (b) Corresponding ESI-MS spectrum. (c) Deconvolution of ESI-MS spectrum.

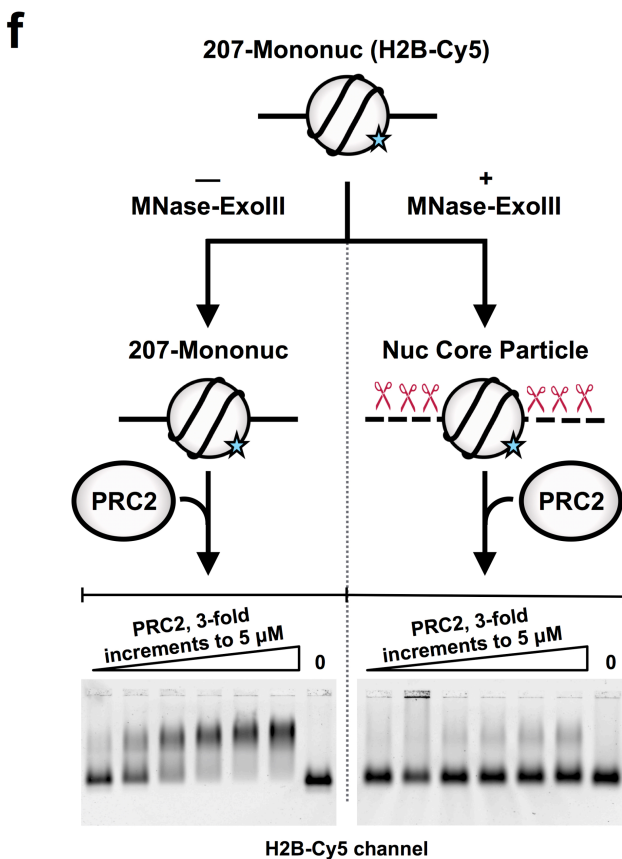
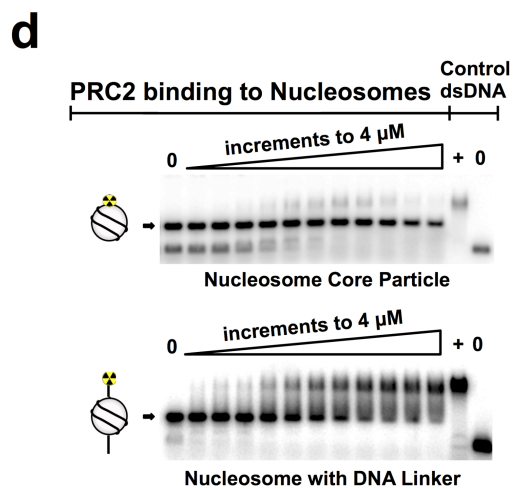
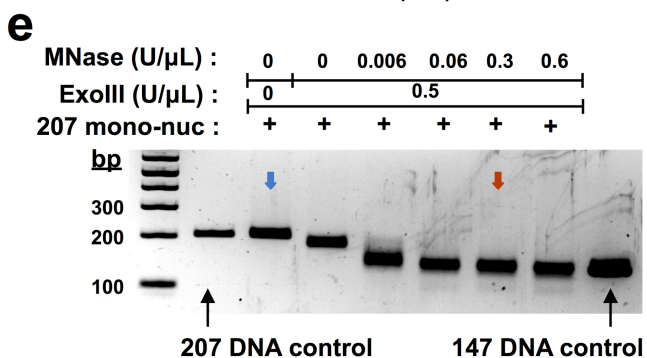
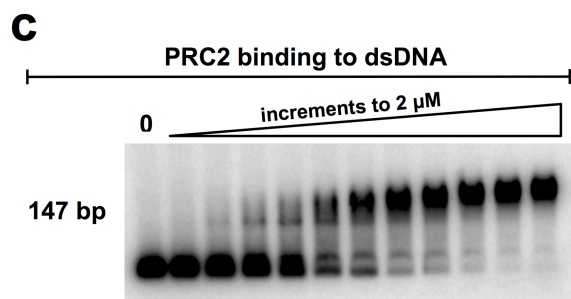
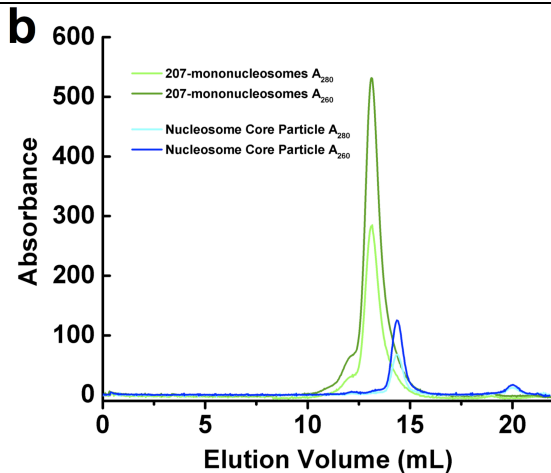
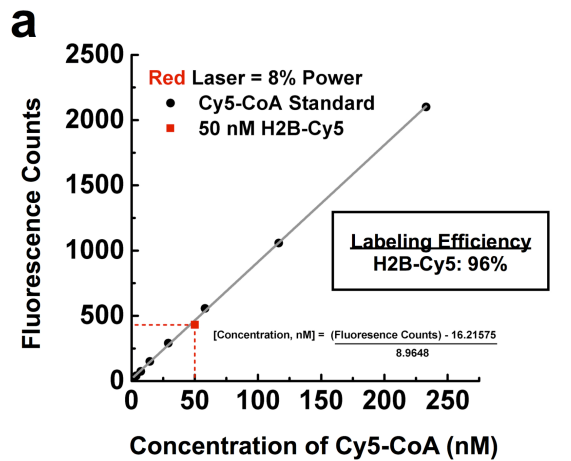


## Supplementary Figure 4

### RNA strips PRC2 away from modified nucleosomes, Related to Figure 2.

(a) The elution profile of H3K27me3-histone octamer is similar to unmodified histone octamer. Only fractions ranging from 68–72 mL (highlighted on the chromatogram curve), where histone subunits were stoichiometric with one another (1:1:1:1), as determined by SDS-PAGE, were collected, pooled, and used for reconstitution experiments. Elution profiles for other modified-histone octamers were similar (data not shown) (b) Equilibrium binding curves for EMSA data of PRC2 binding to modified mononucleosomes. (c) (GGAA)<sub>10</sub> RNA disrupts pre-formed complexes of PRC2-H3K27M-trinucleosome and PRC2-H3K4me3-trinucleosome, indicating that neither histone marks nor a cancer mutation impact the regulatory role of RNA *in vitro*. All PRC2-trinucleosome complexes were fully disrupted (indicated by a red arrow) at a PRC2:RNA molar ratio of ~2:1. Data points represent 2-fold titrations ranging from 0–10 μM RNA. (d) EMSA gels of PRC2 binding to protein-free 207 bp and 621 bp dsDNA templates. Data points represent 2-fold titrations ranging from 0–1 μM PRC2.

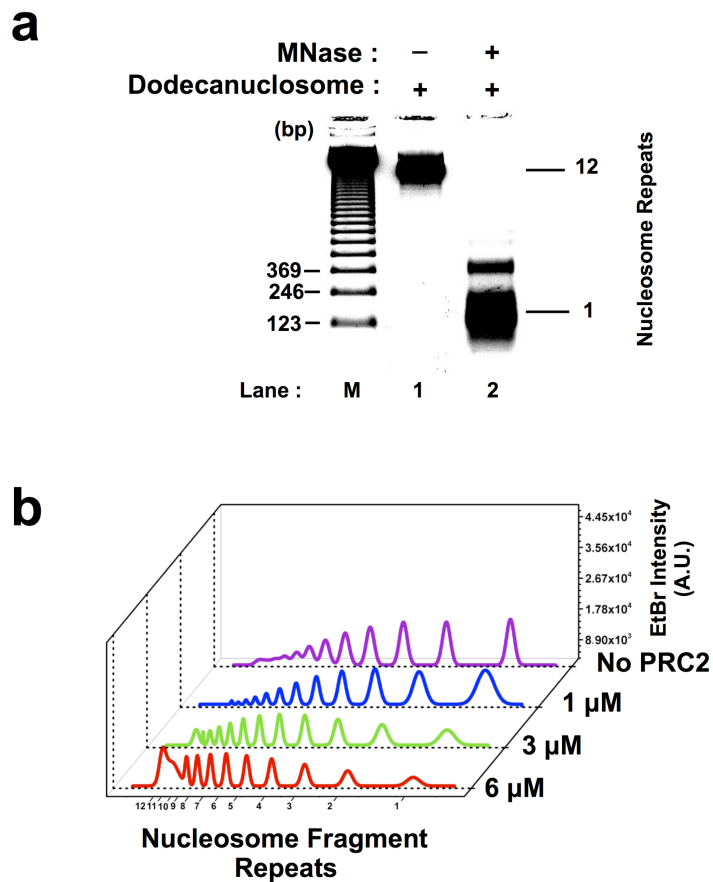




## Supplementary Figure 5

Removing linker DNA from nucleosomes attenuates nanomolar binding affinity, Related to Figure 3.

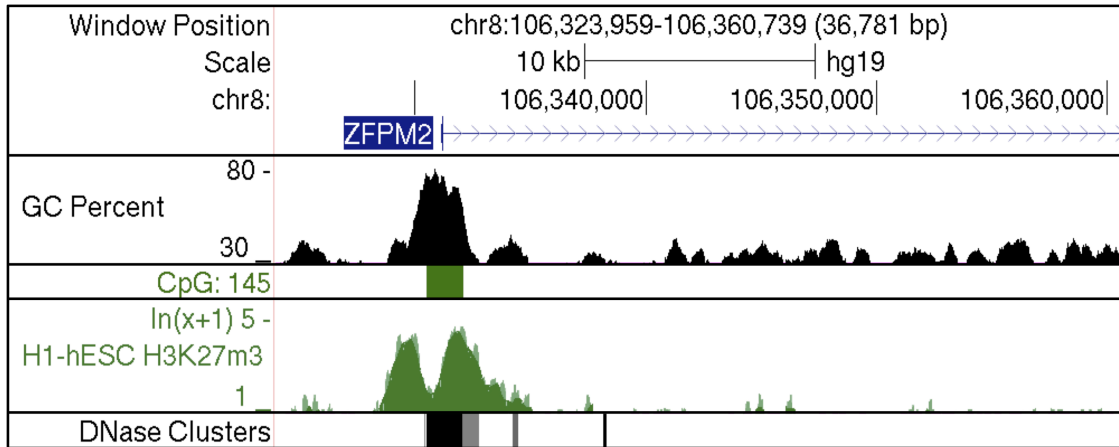
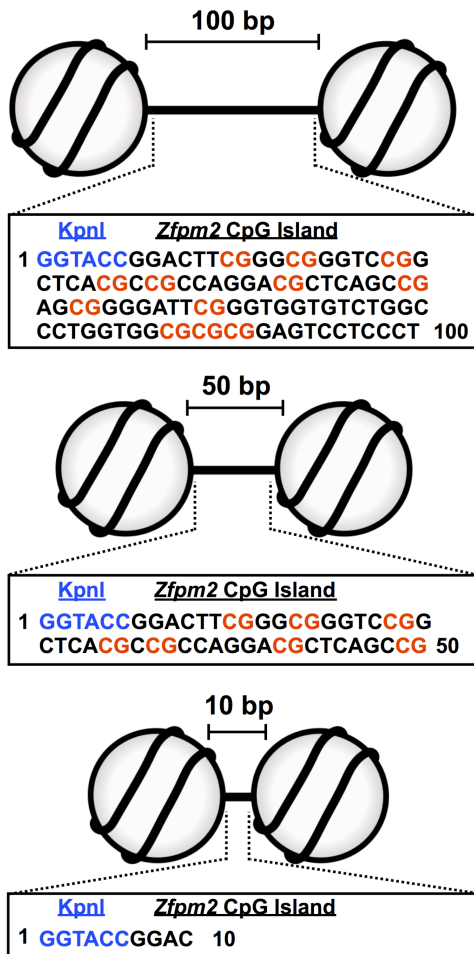
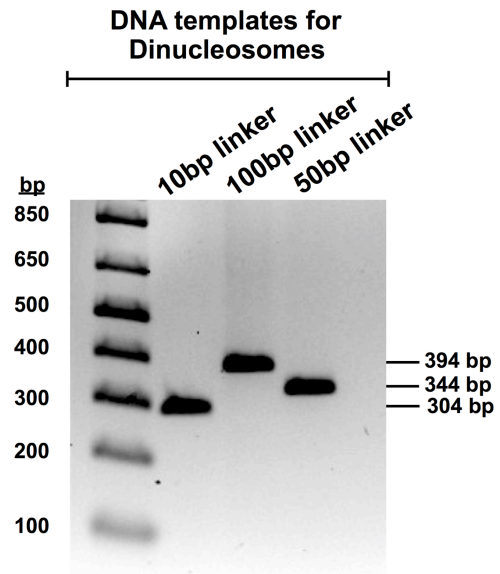
(a) Labeling efficiency of H2B-Cy5 is 96%, as determined using a Cy5-CoA calibration curve. Fluorescence signal was counted using an MST instrument (NanoTemper). (b) Fractionation of mononucleosome and nucleosome core particles on a Superose 6 Increase column show that reconstituted nucleosomes are homogenous and monodisperse and lack contaminating free DNA. (c) EMSA gel of PRC2 binding to protein-free 147 bp dsDNA template. Data points represent 2-fold titrations ranging from 0–2  $\mu$ M PRC2. (d) EMSA of PRC2 binding to  $^{32}$ P-radiolabeled nucleosome substrates. Nucleosome core particles lacking an accessible DNA linker attenuated PRC2 binding. Nanomolar binding affinity to nucleosomes was restored by the addition of a linker DNA. Data points represent 2-fold titrations ranging from 0–4  $\mu$ M. (e) Trimming of 207 bp mononucleosomes to nucleosome core particles was performed by MNase-ExoIII digestion. Following treatment of 207 mononucleosomes with MNase-ExoIII, aliquots were taken from each sample and proteinase K-treated to remove histone proteins. DNA were then purified and run on agarose gel. DNA was visualized by EtBr staining. Blue arrow indicates untrimmed-207 mononucleosome. Red arrow indicates fully trimmed-207 mononucleosome DNA. (f) PRC2 binding to mononucleosomes with and without MNase-ExoIII treatment shows that PRC2 nanomolar binding affinity to nucleosomes is due to linker DNA binding.



**Supplementary Figure 6**

PRC2 binds accessible DNA regions of nucleosome arrays, Related to Figure 3.

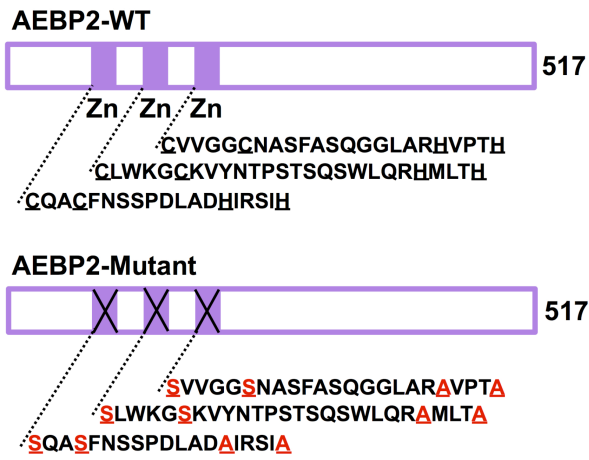
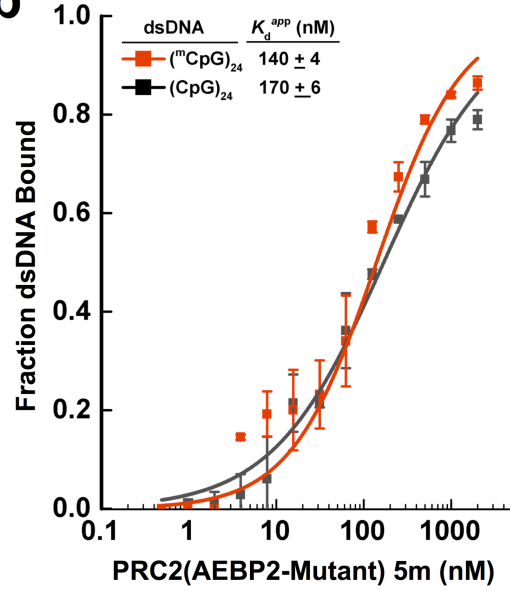
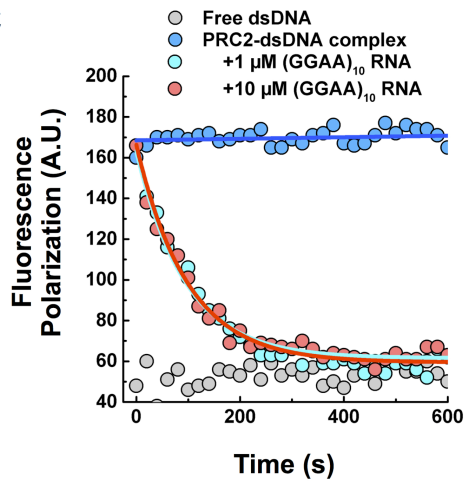
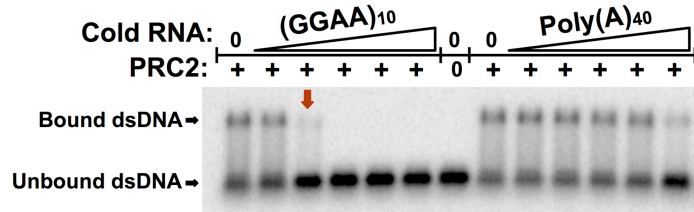
(a) MNase limit digestion shows that prolonged MNase treatment of dodecanucleosomes results in a mostly mononucleosome species. (b) Quantifications of Fig. 3c (lanes 1–4).

**a****b****c**

## Supplementary Figure 7

### Design of a promoter dinucleosome mimic, Related to Figure 4.

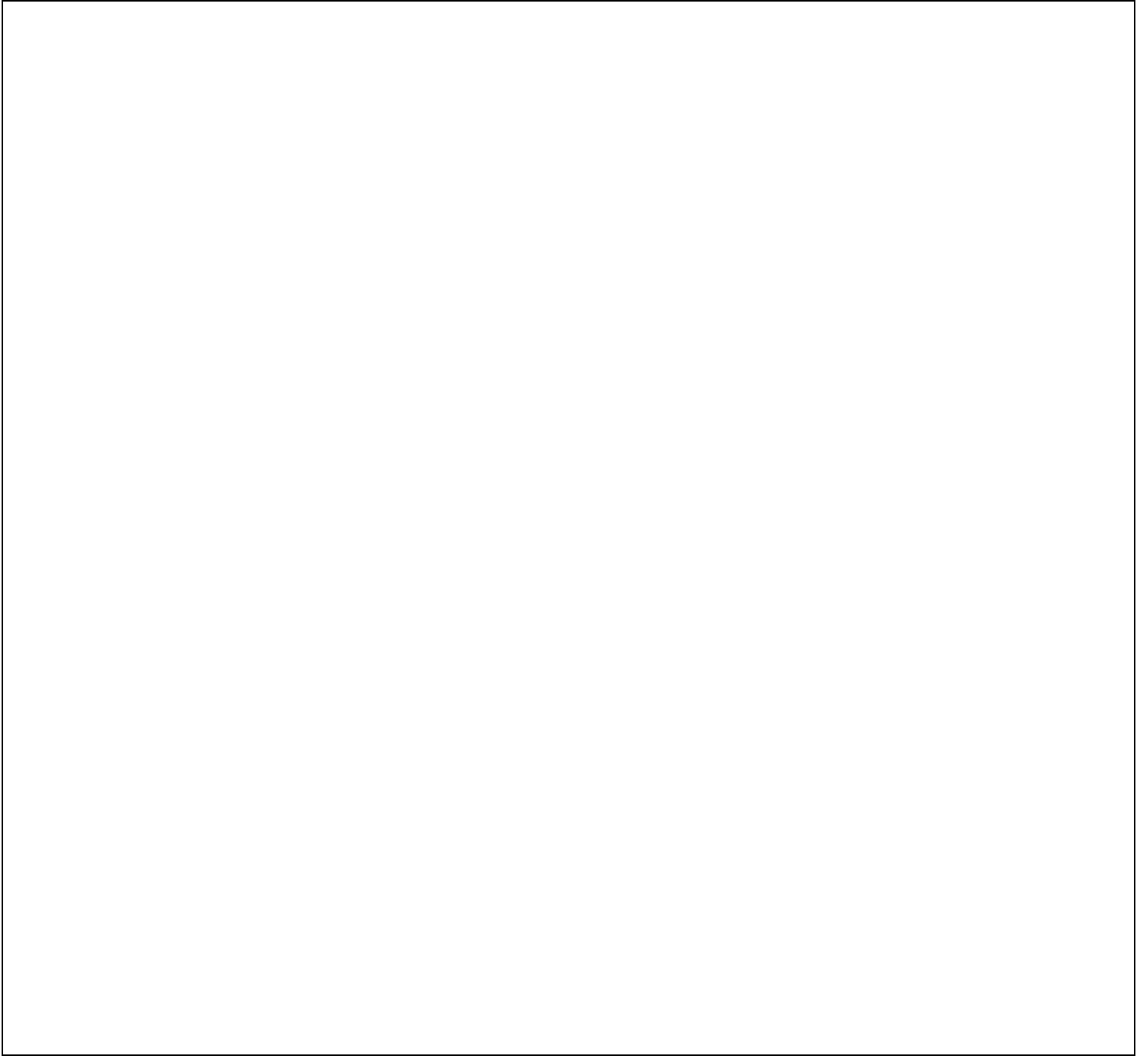
(a) Genome browser snapshot of the human *ZFPM2* gene showing the regional GC percent, the log<sub>2</sub> ratio enrichment for H3K27me<sub>3</sub> in H1-hESC cell line, and regional DNase hypersensitive clusters. (b) Design of dinucleosome mimics from the *ZFPM2* promoter. The linker sequence adjoining the two nucleosomes is from the promoter CpG island of *ZFPM2*, which shows H3K27me<sub>3</sub> enrichment in ES cells. (c) DNA agarose gel showing the purity of dinucleosome positioning DNA with varying DNA linker (10, 50, and 100 bp) used for the reconstitution of dinucleosomes.

**a****b****c****d**

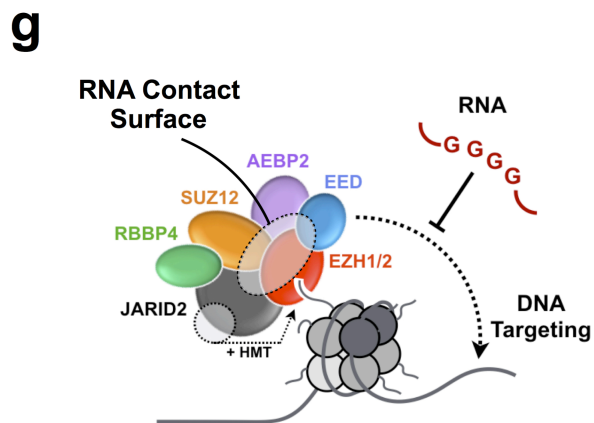
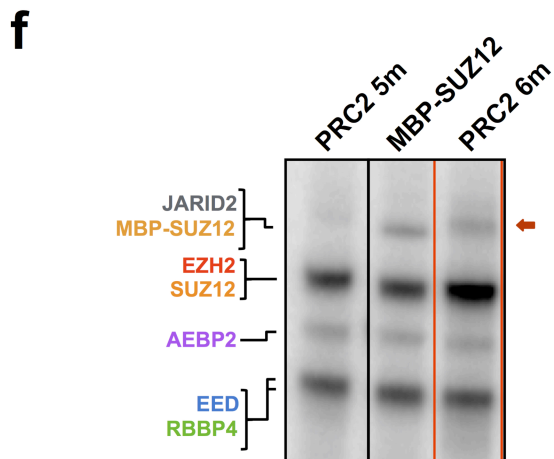
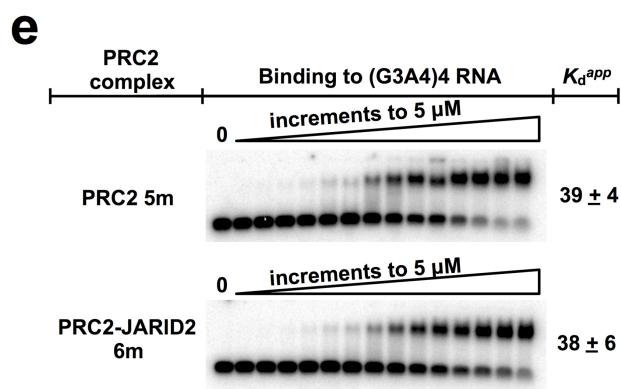
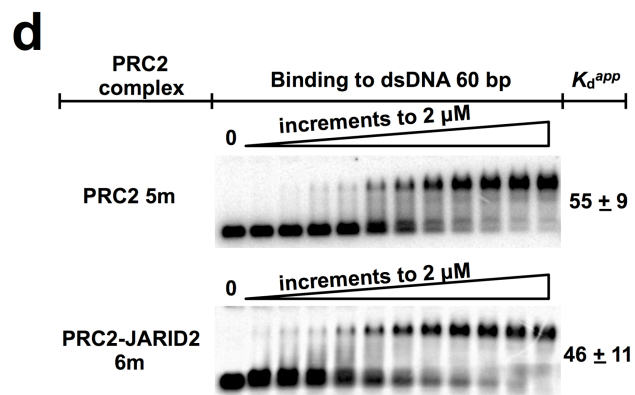
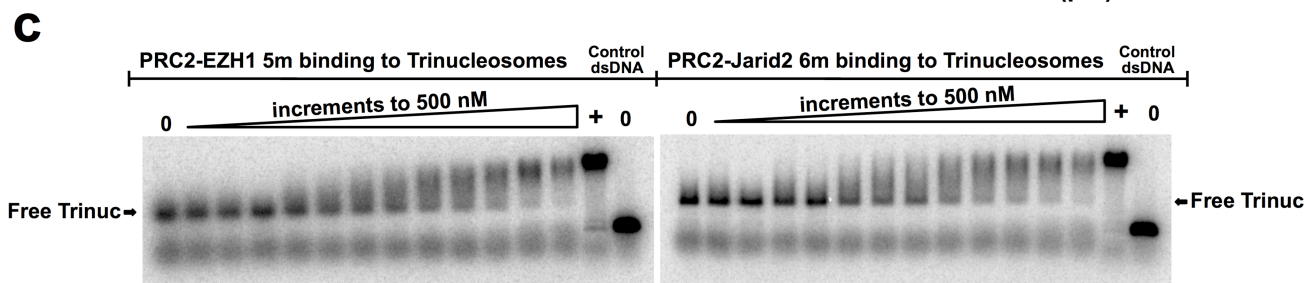
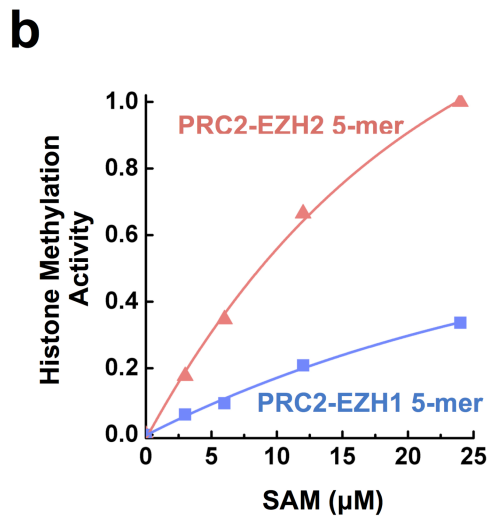
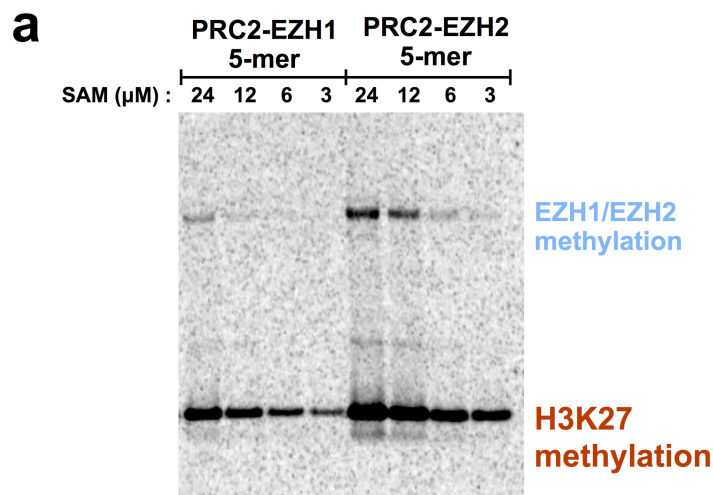
## Supplementary Figure 8

### RNA and DNA bind competitively to PRC2, Related to Figure 5.

**(a)** Schematic representation of the AEBP2 subunit. Mutations introduced to disrupt the three Zinc finger domains in AEBP2 are indicated in red text. **(b)** Equilibrium binding curves appear to suggest that PRC2(AEBP2-Mutant) 5-mer complex lacks recognition of methylated CpG dinucleotides. Error bars give SD,  $n = 3$ . **(c)** Fluorescence polarization assay to measure the dissociation rate of pre-formed PRC2-Alexa488-dsDNA complex in the presence of  $(GGAA)_{10}$  RNA competitor. 5 nM of Alexa488-dsDNA probe was incubated with 200 nM of PRC2 for 30 min before adding 1 or 10  $\mu$ M RNA competitor (200-fold or 2000-fold excess to fluorescent probe). **(d)** Gel-based competition experiment showing that  $(GGAA)_{10}$  RNA competes off PRC2 from pre-formed PRC2-dsDNA complexes, whereas negative control Poly(A)<sub>40</sub> RNA does not compete. RNAs were titrated from 0–10  $\mu$ M in 3-fold increments.



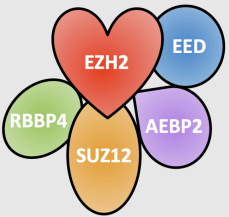
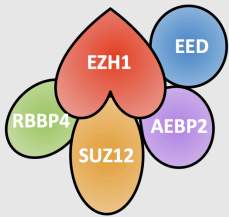
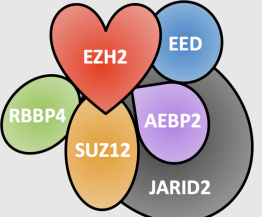




## Supplementary Figure 9

### The JARID2 subunit does not alter trends in DNA and RNA-binding but contributes an RNA-contacting surface, Related to Figure 6.

(a) A comparison of histone methyltransferase activity between PRC2-EZH1 5-mer and PRC2 5-mer using mononucleosome substrates shows that EZH1 has much reduced activity compared to EZH2. Notably, EZH1 appears to be auto-methylated similarly to EZH2. Methylation signal detected by  $^{14}\text{C}$ -autoradiography. (b) Quantification of PRC2-EZH1 5-mer methyltransferase activity. (c) EMSA gels of PRC2 EZH1 5-mer and PRC2-JARID2 6-mer binding to trinucleosome. (d) EMSA gels comparing PRC2 5-mer and PRC2-JARID2 6-mer binding to 60 bp dsDNA. 5 nM of Alexa488-dsNA probe was used. Data points represent 2-fold increments ranging from 0–2  $\mu\text{M}$ .  $K_d^{app}$  in units of nM. SD was calculated from three replicates. (e) EMSA gels comparing PRC2 5-mer and PRC2-JARID2 6-mer binding to G-quadruplex forming (G3A4)<sub>4</sub> RNA. For these RNA binding experiments, binding buffer contained fragmented yeast tRNA competitor, as previously described<sup>8</sup>. Data points represent 3-fold increments ranging from 0–5  $\mu\text{M}$ .  $K_d^{app}$  in units of nM. SD was calculated from three replicates. (f) Cross-linking analysis of 4-U-RNA to PRC2-JARID 6-mer shows that JARID2 is cross-linked to RNA. (g) Model showing the RNA contact region in the PRC2-JARID2 6-mer complex as it spans across five subunits<sup>8</sup>, and the role of JARID2 in allosterically regulating PRC2 activity.

Properties	PRC2-EZH2 5-mer	PRC2-EZH1 5-mer	PRC2-JARID2 6-mer
Subunit Composition	EZH2-EED-SUZ12-RBBP4-AEBP2 	EZH1-EED-SUZ12-RBBP4-AEBP2 	EZH2-EED-SUZ12-RBBP4-AEBP2-JARID2 
Mass (kDa)	320	320	459
Binding to RNA	✓	✓	✓
Binding to Nucleosome Core Particle	✗	✗	✗
Binding to dsDNA	✓	✓	✓
Binding to nucleosomes competed by (GGAA) <sub>10</sub> RNA	✓	✓	✓
Binding to nucleosomes competed by Poly(A) <sub>40</sub> RNA	✗	✗	✗
Methyltransferase Activity	✓	Much Reduced	Enhanced

Supplementary Figure 10

Summary and comparison of biochemical properties of different PRC2 complexes, Related to Figure 7.